

Electronic Supplementary Information

Growth of Well-Ordered Iron Sulfide Thin Films

*Earl Matthew Davis,^a Giulia Berti,^a Helmut Kuhlenbeck,^a Vedran Vonk,^b Andreas Stierle,^{b,c} and
Hans-Joachim Freund^a*

^aFritz-Haber-Institut der Max-Planck-Gesellschaft, Faradayweg 4-6, 14195 Berlin, Germany

^bDeutsches Elektronen-Synchrotron (DESY), 22607 Hamburg, Germany

^cPhysics Department, University of Hamburg, Jungiusstrasse 9, 20355 Hamburg, Germany

CONTENTS

CONTENTS	1
1. THIN FILM GROWTH ON Pt(001)	2
SI Figure 1. LEED images and TPD spectrum of iron sulfide film on Pt(001)	4
SI Figure 2. XPS survey spectra showing the increase in Pt signal following annealing	4
2. XRD DATA	4
SI Table 1. Observed and calculated structure factors for the reflections	5
SI Figure 3. The NiAs-like structure model	5
3. LEED-I/V CALCULATIONS	5
SI Table 2. R-factors for LEED-I/V calculations performed using models with bulk-like greigite terminations	7
SI Figure 4. The Fe ₃ S ₄ (111) unit cell	7

SI Table 3. R-factors for LEED-I/V calculations performed using models with bulk-like pyrite FeS ₂ (111) terminations	7
SI Figure 5. I/V-curves from the reconstructed greigite-like surface.....	9
REFERENCES	10

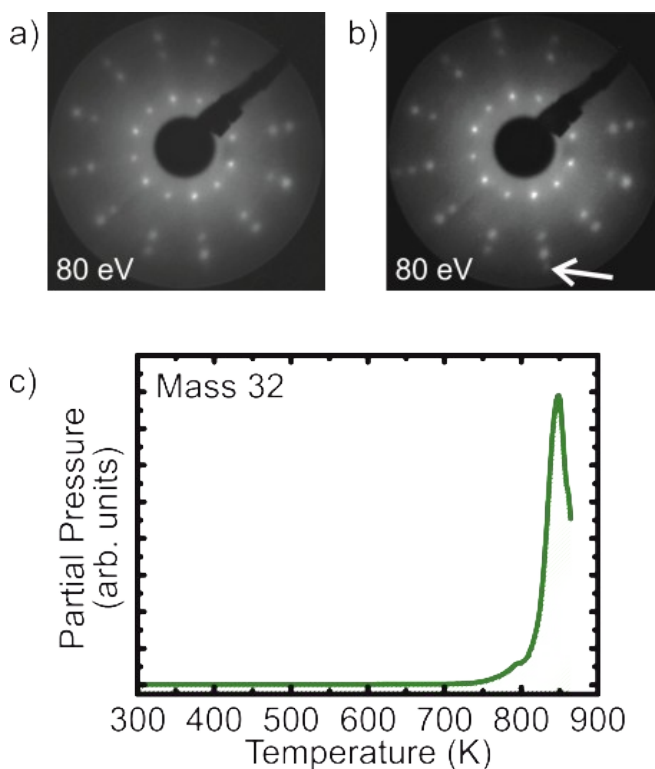
1. THIN FILM GROWTH ON Pt(001)

The substrate was prepared via cycles of Ar⁺ sputtering followed by annealing at 1200 K until the Pt-hex reconstruction was visible in the low energy electron diffraction (LEED) pattern. The film was then grown using an Fe deposition rate of 1.65 Å/min and a current across the sulfur cell of I_S = 15 mA for 30 min. The sulfur partial pressure in the deposition chamber rose to 1.5×10⁻⁶ mbar during the film deposition and the sample was kept at 625 K throughout. Fe and S deposition were ended simultaneously. This procedure resulted in an iron sulfide film with a LEED pattern as shown in Figure 1a, showing 2 hexagonal rotational domains above a large background intensity.

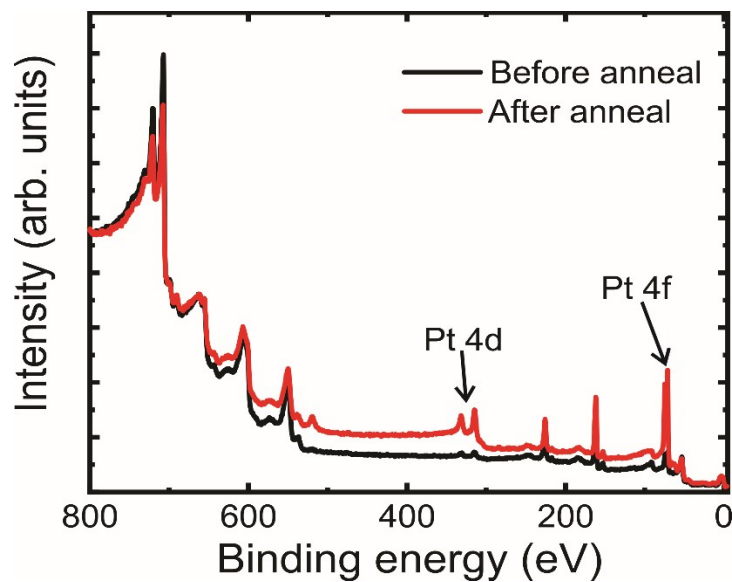
Following annealing of the film at 750 K for 3 minutes, additional diffraction spots became faintly visible in the LEED pattern as indicated by the arrow in Figure 1b, with marginal reduction in background intensity. These spots were found at the same position as the main spots from the Pt(001) LEED pattern. Additionally, XPS spectra (Figure 2) revealed a large increase of the Pt signal. It was concluded that the film had dewetted, and therefore the additional spots in the LEED pattern were assigned to the substrate. The substrate spots are ~2.5 times further from the centre of the LEED pattern than the central LEED spots from the film. This allows us to estimate that the surface lattice parameter of the hexagonal film is ~7 Å.

The decomposition of the iron sulfide film was investigated by using the QMS to measure sulfur desorption from the sample as it was heated at a rate of 0.5 K/s. Partial pressure at mass

32, corresponding to S atoms, as a function of temperature are shown in Figure 1c, with a large peak at ~ 850 K. The increase in the desorption rate of sulfur begins in earnest at ~ 750 K, giving an upper temperature limit for non-destructive annealing. Although mass 32 could also correspond to O_2 molecules, this desorption rate was mirrored in the data from mass 64, corresponding to S_2 molecules. Despite annealing the iron sulfide film at lower temperatures, XPS showed an increase in the signal from Pt. It was also not possible to improve the ordering of the film, as judged by the LEED pattern.



SI Figure 1. LEED images after (a) iron sulfide film growth on Pt(001) and (b) annealing at 750 K for 3 min. The arrow in (b) indicates the position of one of the four visible substrate spots. (c) Desorption of S from the iron sulfide film as a function of temperature. The LEED images have been brightened for clarity.

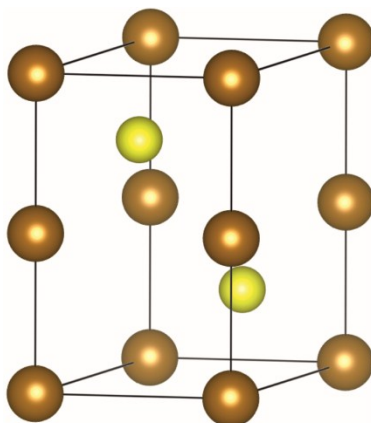


SI Figure 2. XPS survey spectra showing the increase in Pt signal following annealing at 750 K for 3 minutes.

2. XRD DATA

Reflection	F_{obs}	dF	F_{calc}	$ F_{\text{calc}} - F_{\text{obs}} / F_{\text{obs}}$
(100)	280.92	42.60	177.34	0.37
(110)	463.69	36.90	527.98	0.14
(200)	136.26	20.44	112.28	0.18
(101)	215.25	15.10	190.50	0.11
(201)	115.02	10.60	118.65	0.03
(102)	327.44	82.70	335.89	0.03
(112)	53.89	8.08	56.29	0.04
(202)	174.39	40.70	220.11	0.26

SI Table 1. Observed structure factors for the reflections, F_{obs} , their error, dF , and the calculated value of the structure factor for the NiAs structure model, F_{calc} . The final R-value for the model is $R = 0.157$. The model structure is shown in SI Figure 3.



SI Figure 3. The NiAs-like structure providing the best fit in structural refinement using the XRD data. The Fe occupancy is 74 %. Brown and yellow spheres represent Fe and S atoms respectively.

3. LEED-I/V CALCULATIONS

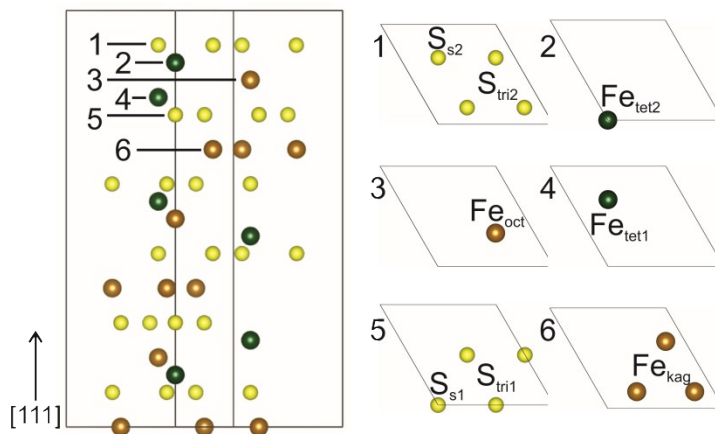
For initial LEED-I/V measurements, spots were tracked in the energy range 50-350 eV. The spots were divided into 7 groups of symmetrically inequivalent spots, with a total energy range of 1212 eV. The muffin tin radii for the calculation of phase shifts were 1.7 Å for both Fe and S atoms. In addition to positional parameters, Debye temperatures and the imaginary part of the inner potential were also optimised for model surface structures. For calculations using greigite, the lattice parameter and the positional parameter u were also optimised. In order to produce the symmetry observed in the experimental LEED-I/V curves, the calculated intensity curves from models with lower symmetry were averaged to simulate the presence of the appropriate rotational domains.

The R-factors for calculations using bulk-like terminations of greigite are given in SI Table 2, with the lowest R-factor coming from the S_{s2} termination. For pyrite, there were four

terminations that could produce an arrangement like that seen in STM, and these are presented in SI Table 3.

Termination	Best R-factor
Fe _{kag}	0.383
Fe _{tet1}	0.364
Fe _{oct}	0.617
Fe _{tet2}	0.427
S _{s2}	0.272
S _{s1}	0.342

SI Table 2. R-factors for LEED-I/V calculations performed using models with bulk-like greigite terminations. For the layer names refer to SI Figure 4.



SI Figure 4. The Fe₃S₄(111) unit cell, with the top view of layers 1-6 showing the naming conventions used here for the atoms. Layers 1-6 are repeated, shifted laterally to lie around different rotational centres within the unit cell.

Termination	Best R-factor
Fe	0.502
Single S atom above Fe layer	0.464
Double S layer	0.499
Between the two S layers	0.556

SI Table 3. R-factors for LEED-I/V calculations performed using models with bulk-like pyrite $\text{FeS}_2(111)$ terminations.

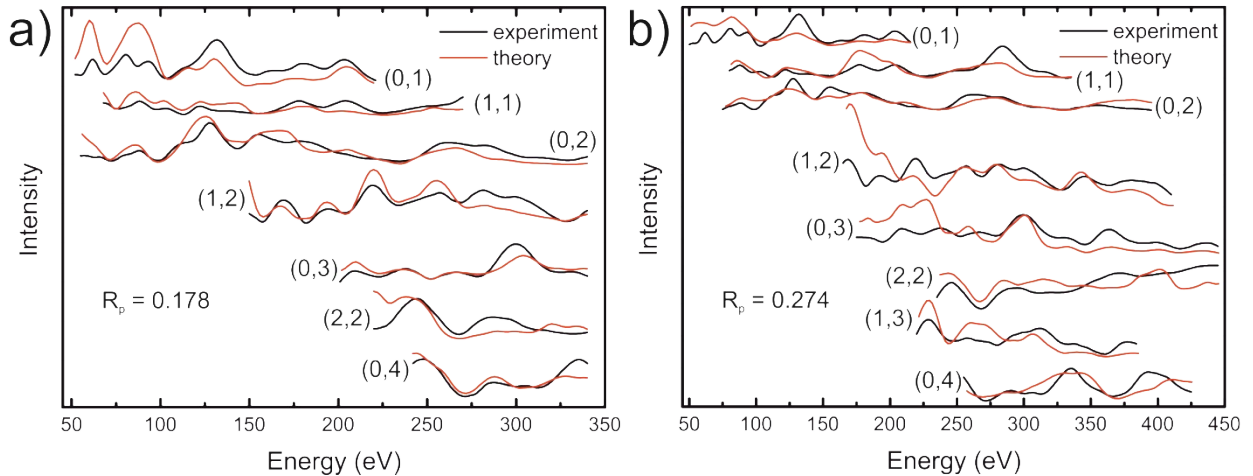
Hexagonal pyrrhotite was modelled using the $\text{Fe}_7\text{S}_8\text{-3C}$ structure given by Nakano et al. [1]. Bulk terminations containing 3 or 4 sulfur or iron atoms were considered. The best R-factor, came from the layer terminated by 4 sulfur atoms, with $R_p = 0.416$.

The NiAs structure of the high temperature form of FeS was used as a model structure. A 2×2 reconstruction was simulated by combining four unit cells into one 2×2 unit cell, and the atoms at high symmetry positions within the expanded unit cell were displaced vertically relative to the rest of the layer. The best result came from a sulfur terminated layer giving a best R-factor of $R_p = 0.447$.

For smythite, a 2×2 reconstruction was simulated in the same way as described above for FeS. The best R-factors were produced for models of the bulk-like termination between consecutive sulfur layers, with a minimum of $R_p = 0.226$.

Having tried these bulk-like terminations, various reconstructions were used as model structures. Bulk-like greigite terminations were among the model structures achieving the lowest R-factors, so these were some of the candidates for reconstruction. We experimented with changing the sequence of the terminating greigite layers, however this was without improvement in the R-factor. Calculations performed by Roldan and de Leeuw found that $\text{Fe}_3\text{S}_4(111)$

optimally terminated at either an Fe_{oct} or Fe_{kag} layer [2]. Following relaxation, the terminating Fe atoms moved into the subsurface, leaving a sulfur termination and an accumulation of Fe beneath the sulfur layer. This suggests a tendency for accumulation of Fe in the subsurface region. A film with layers 5 and 6 (as labelled in SI Figure 2) repeated as the terminating layers was trialled, with a layer 4 placed alongside the uppermost layer 6. This resulted in an R-factor of $R_p = 0.178$. The comparison of the experimental and theoretical curves is presented in SI Figure 5a. Extending the dataset to a range of 50-500 eV gave a total range of data from symmetrically inequivalent spots of 1807 eV. Over this energy range, the search procedure for the above structure was again performed, however the best R-factor achieved was $R_p = 0.274$, with the comparison of the curves shown in SI Figure 5b. This shows that the model does not accurately reflect the surface structure of the film because the model does poorly at predicting the curves outside of the initial fitting range, though there may be aspects which closely resemble the true structure.



SI Figure 5. I/V-curves from the reconstructed greigite-like surface (a) giving an R-factor of 0.178 for a total fitting range of 1212 eV, and (b) over an extended range of 1807 eV giving an R-factor of 0.272. The indexing of the spots is relative to the surface unit cell.

Potential 2×2 reconstructions of the NiAs-like structure described in the main text were trialled, using the extended energy range. Reconstructions were simulated by introducing Fe vacancies (from an FeS stoichiometry), reordering of the stacking sequence, and laterally shifting layers to different centres of rotational symmetry. The best R-factor was achieved for a sulfur-terminated bulk-like film without vacancies, where the bulk z-coordinate of the sulfur atoms placed them closer to the Fe atoms below the S layer (than to the Fe atoms above). The R-factor this structure gave was $R_p = 0.333$.

REFERENCES

- [1] A. Nakano, M. Tokonami, N. Morimoto, Refinement of 3C pyrrhotite, Fe₇S₈, *Acta Crystallogr. Sect. B Struct. Crystallogr. Cryst. Chem.* 35 (1979) 722–724. doi:10.1107/S0567740879004532.
- [2] A. Roldan, N.H. de Leeuw, Catalytic water dissociation by greigite Fe₃S₄ surfaces: density functional theory study, *Proc. R. Soc. A Math. Phys. Eng. Sci.* 472 (2016) 20160080. doi:10.1098/rspa.2016.0080.